Development of a Mechanistic Model for Biological Nutrient Removal Activated Sludge Systems and Application to a Full-Scale WWTP

Bing-Jie Ni, Wen-Ming Xie, Shao-Gen Liu, and Han-Qing Yu
Dept. of Chemistry, University of Science and Technology of China, Hefei, P.R. China

Yi-Ping Gan, Jun Zhou, and Er-Cheng Hao
Beijing Drainage Group Ltd., Beijing, P.R. China

DOI 10.1002/aic.12066
Published online September 16, 2009 in Wiley InterScience (www.interscience.wiley.com).

In wastewater treatment plants (WWTPs) the production of nitrite as an intermediate in the biological nutrient removal (BNR) process has been widely observed, but not been taken into account by most of the conventional activated sludge models yet. This work aims to develop a mechanistic mathematical model to evaluate the BNR process after resolving such a problem. A mathematical model is developed based on the Activated Sludge Model No.3 (ASM3) and the EAWAG Bio-P model with an incorporation of the two-step nitrification–denitrification, the anoxic P uptake, and the associated two-step denitrification by phosphorus accumulating organisms. The database used for simulations originates from a full-scale BNR municipal wastewater treatment plant. The influent wastewater composition is characterized using batch tests. Model predictions are compared with the measured concentrations of chemical oxygen demand (COD), NH_4^+-N, NO_2^--N, NO_3^--N, PO_4^{3-}-P, and mixed liquid volatile suspended solids. Simulation results indicate that the calibrated model is capable of predicting the microbial growth, COD removal, nitrification and denitrification, as well as aerobic and anoxic P removal. Thus, this model can be used to evaluate and simulate full-scale BNR activated sludge WWTPs. © 2009 American Institute of Chemical Engineers *AIChE J,* 56: 1626–1638, 2010

Keywords: biological nutrient removal (BNR), denitrification, modeling, nitrification, nitrite, phosphorus, wastewater treatment plant (WWTP)

Introduction

In activated sludge processes for municipal wastewater treatment plants (WWTPs) the biological removal of nitrogen, phosphorus, and organic carbon substances can be simultaneously achieved. The phosphorus-removing process is more complex, compared with the N- and chemical oxygen demand (COD)-removing processes.[1–5] Mathematical modeling has been demonstrated to be essential to understand the complex microbial systems, such as a biological nutrient removal (BNR) activated sludge system.[6,7] In addition, dynamic simulation of a WWTP is also found to be useful for selecting operational strategies to improve process stability, effluent quality and save operational costs.[8,9]

Optimum solutions to the design and operation of a WWTP should include the mutual relationship among the different process elements involved in wastewater and activated sludge. Furthermore, a model regarding WWTP should be also able to

Correspondence concerning this article should be addressed to H.-Q. Yu at hqyu@ustc.edu.cn.

transform the data obtained from lab-scale experiments into quantitative knowledge, which helps in decision-making processes.[10,11] Therefore, when a model is developed to simulate a BNR WWTP, a comprehensive description of all the relevant processes in the BNR should be taken into account.

Various types of models, such as the white-box model, have been widely applied in this field, with learning, design, and process optimization as the main applications.[11] The Activated Sludge Models (ASMs) developed by the International Water Association task group, such as Activated Sludge Model No.1 (ASM1) and No.3 (ASM3),[12] focus on the heterogeneity of substrate and biomass types, and are suitable for simulating a full-scale WWTP. The introduction of the ASM model family is of great importance, as they provide researchers and practitioners with a standardized set of basis models. The ASM models, which integrate knowledge, could also be used for many purposes, e.g., for the development of virtual activated sludge processes.

The ASM1 was developed primarily for municipal treatment plants to simulate the removal of organic carbon and ammonium-N,[13] while the subsequent ASM3 was established to sort out a number of problems that have emerged from the applications of ASM1.[12,14] The new point of ASM3 with respect to ASM1 is a real change in the modeling paradigm from the maintenance/death/regeneration concepts to the storage components. In ASM3, the storage of organic substrates is included as a new process and lysis is replaced by an endogenous respiration process. As a result, the hydrolysis becomes less important for the rates of oxygen consumption and denitrification, and becomes independent of the electron donor, compared with ASM1. Furthermore, the rates of all processes (except for hydrolysis) under anoxic conditions are lower than those under aerobic conditions. In ASM3 smaller anoxic yield coefficients are used.[14] ASM1 has been used as a tool for modeling the removal of organic matter and for nitrification and denitrification processes for more than a decade; considerable experience with this model has been acquired. However, it is a different case for ASM3, as it has not been extensively validated, attributed to the fact that the model became available only recently.

ASM3 is a basic model, which can be used to predict oxygen consumption, sludge production, nitrification, and denitrification in activated sludge for the treatment of municipal wastewater.[12] Biological phosphorus removal process is not taken into account in ASM3. To sort out this problem, the EAWAG Bio-P model was proposed to add biological phosphorus removal into a calibrated version of ASM3.[15] The revised ASM3 is extended by terms for phosphorus limitations in the microbial growth processes, but almost all of processes and parameters are the same to those in ASM3.[14,15] The EAWAG Bio-P model was designed without an additional glycogen pool, because previous studies had shown no significant influence of glycogen on the biological phosphorus removal.[15] However, kinetics of nitrification–denitrification and denitrifying phosphorus removal in these models are assumed as single-step processes. It is not true for some cases, where a considerable amount of nitrite is observed to build-up in full-scale BNR WWTPs. This is a limitation of the ASMs and their extended versions. In this case, a modeling tool could be useful to anticipate the nitrite peaks, change control strategies or operational conditions.[16]

In the nitrification process, the transformation from ammonium to nitrate occurs in two steps with nitrite as an intermediate. With the increasing application of nitrification-including processes, modeling of nitrite in the two-step nitrification has been commonly used and well documented.[5,16] On the contrary, nitrite is often neglected in modeling denitrification processes and only few attempts have been made to incorporate the intermediate in the existing models.[17]

The BNR activated sludge system has been widely used for municipal wastewater treatment. As an aid for its application, a mathematical simulation model for BNR would be a useful tool. Therefore, the main objective of this study is to develop a mechanistic model for the BNR processes in full-scale WWTP, based on the ASM3 and the EAWAG Bio-P model with significant modifications. After incorporating the two-step nitrification–denitrification, the anoxic P uptake, and the two-step denitrifying phosphorus removal, the developed model can be applied to simulate and describe the performance of a full-scale anaerobic-anoxic-aerobic WWTP.

Model Development

General descriptions

The ASM3 model and the EAWAG Bio-P model are the foundation of our model.[14,15] In our work, the two models are combined and extended through taking two-step nitrification–denitrification, anoxic P uptake, and associated two-step denitrification by phosphorus accumulating organisms (PAOs) into account. For this mathematical model for BNR, the model components, biological processes, kinetic rate equations, and their stoichiometric interactions with components are presented in matrix format throughout Tables 1–6.

The symbol system in ASMs is followed and appropriately supplemented in the model development,[12] as shown in Table 1. Related process kinetics and stoichiometrics to describe the interactions and transformations among model components are expressed compatibly with other ASMs.[12] The process rate expressions for ordinary heterotrophic organisms (X_H), ammonia-oxidizing organisms (AOB, X_{AOB}), nitrite-oxidizing organisms (NOB, X_{NOB}), and phosphorus accumulating organisms (X_{PAO}) are given in Table 2, reflecting the basic kinetic relationships constituting the model backbone. The relevant stoichiometric coefficients for these microorganisms are incorporated in appropriate matrix cells of Tables 3–5, with Table 3 for X_H, Table 4 for X_{AOB} and X_{NOB}, and Table 5 for X_{PAO}. The changing rate (generation or utilization) of a model component for a given biochemical process can be obtained through multiplication of related process stoichiometrics and kinetics.[18,19] Suggested values for the kinetic and stoichiometric parameters are listed in Table 6, which defines all the parameters used in the developed model, their symbols, and their units.

Model components

To develop a mechanistic model for simulating full-scale WWTP with the removal of COD, nitrogen, and phosphorus from municipal wastewater, wastewater and activated sludge need to be characterized. In our model, there are 11 COD components identified for carbonaceous materials, four

Table 1. Definition of Components in the Developed Model

Number	Component	Definition	Unit
Model dissolved components			
1	S_O	Dissolved oxygen	g O_2 m^{-3}
2	S_S	Readily biodegradable substrate	g COD m^{-3}
3	S_I	Inert, non-biodegradable organics	g COD m^{-3}
4	S_{NH4}	Ammonium nitrogen	g N m^{-3}
5	S_{NO_3}	Nitrate nitrogen	g N m^{-3}
6	S_{NO_2}	Nitrite nitrogen	g N m^{-3}
7	S_{N_2}	Dissolved nitrogen	g N m^{-3}
8	S_{PO_4}	Phosphate phosphorus	g P m^{-3}
Model particulate components			
9	X_H	Active ordinary heterotrophic organisms	g COD m^{-3}
10	X_{AOB}	Active ammonia-oxidizer bacteria	g COD m^{-3}
11	X_{NOB}	Active nitrite-oxidizer bacteria	g COD m^{-3}
12	X_{PAO}	Active phosphorus accumulating organisms	g COD m^{-3}
13	X_{STO}	Storage polymers of X_H	g COD m^{-3}
14	X_{PHA}	Stored polyhydroxyalkanoate (PHA) of X_{PAO}	g COD m^{-3}
15	X_{PP}	Stored polyphosphate of X_{PAO}	g P m^{-3}
16	X_S	Slowly biodegradable substrate	g COD m^{-3}
17	X_I	Inert, non-biodegradable organics	g COD m^{-3}

components for nitrogenous materials and two components for phosphorus materials in wastewater and activated sludge mixed liquor (Table 1).

The total influent COD can be divided into four fractions: un-biodegradable particulate COD (X_I), un-biodegradable soluble COD (S_I), readily biodegradable COD (S_S), and slowly biodegradable COD (X_S). In contrast to the ASM2d,[20] the fermentation of the readily degradable substrate is neglected in our model, as experimental results demonstrate that there is no limitation of P-release attributed to the fermentation in municipal wastewater.[15,21,22]

For modeling purposes, microorganisms with a particular function are grouped together as a single entity. Thus, active biomass is divided into: ordinary heterotrophic organisms (X_H) being unable to accumulate polyphosphate; ammonia-oxidizing organisms (X_{AOB}) performing nitritation, nitrite-oxidizing organisms (X_{NOB}) performing nitratation, and polyphosphate-accumulating organisms (X_{PAO}) being able to removal phosphate. In addition, there are three internally stored carbonaceous compounds, which play important roles in BNR systems: storage polymers of X_H (X_{STO}), PHA (X_{PHA}), and stored polyphosphate (X_{PP}).

Influent nitrogenous materials include ammonia (S_{NH4}), nitrite (S_{NO2}), nitrate (S_{NO3}), and organic nitrogen contained in the relevant corresponding COD fractions. In our work, nitrite is also included as a separate nitrogen component, as a significant level of nitrite has been observed in many cases.[23–25] Nitrite may accumulate in the two-step nitrification or denitrification processes, and accordingly is considered as an independent component in this model.

Total influent phosphorus materials consist of soluble inorganic P and organic P. Similar to the organic N components given earlier, a fixed organic P content is included in each COD component and hence organic P components are unnecessary for direct inclusion in the model.[26] All soluble inorganic P is considered as phosphate, which is included as a separate component (S_{PO_4}). Furthermore, polyphosphate (X_{PP}) internally stored by PAOs is included as a separate model component.

Biological processes

Hydrolysis. In our model, slowly biodegradable substrate, X_S, is hydrolyzed with a rate characterized by surface reaction kinetics as in ASM models (Process 1 in Table 2). The hydrolysis process is presumably rate limiting for partial utilization processes of readily biodegradable substrate.

Ordinary Heterotrophic Organisms (X_H). Ordinary heterotrophic organisms (X_H) can grow with oxygen, nitrite, or nitrate as an electron acceptor. In the ASM3 model the sole substrate for their growth is storage polymers (X_{STO}).[14] The growth processes, rate equations and their stoichiometric interactions with the components are shown in Tables 2 and 3 (Processes 2–11) with several modifications, compared with ASM3. In the ASMs, one-step complete denitrification (i.e., from NO_3^- to nitrogen gas) is assumed, using Monod kinetics for growth. For instance, in ASM3 denitrification is modeled as a single-step process, neglecting nitrite as the intermediate product. Such an assumption is not reasonable when a considerable amount of nitrite is build up in the system.[24,25] Therefore, in all the anoxic processes of our model, the facultative heterotrophs can remove organic carbon through anoxic respiration on either nitrite or nitrate, which serves as an electron acceptor in the absence of dissolved oxygen (DO). Thus, there are now two separate denitrification rates for the denitrifiers, one on nitrite-N and another on nitrate-N. This generates two separate kinetics for the anoxic storage (Processes 3 and 4), the anoxic growth on X_{STO} (Processes 6 and 7), the anoxic endogenous respiration of active heterotrophs (Process 9), and the anoxic endogenous respiration of X_{STO} (Process 11). Furthermore, denitrification is modeled following a sequential reduction path for oxidized nitrogen species, i.e., nitrate denitrified to nitrite and nitrite denitrified to nitrogen, to better simulate the nitrite accumulation in two-step denitrification processes. In addition, limitations for phosphorus in all growth processes are included in the mechanistic model.

Ammonia Oxidizers and Nitrite Oxidizers. Biological nitrification process can be divided into two steps: ammonia oxidation to nitrite by ammonia oxidizers (AOB), namely

Table 2. Process Kinetic Rate Equations in the Developed Model

Process	Process Rate Equations
1. Hydrolysis	$k_H \frac{X_S/X_H}{K_X+X_S/X_H} X_H$
Ordinary heterotrophic organisms	
2. Aerobic storage	$k_{\mathrm{STO}} \frac{S_S}{K_{S,H}+S_S} \frac{S_{\mathrm{O_2}}}{K_{H,\mathrm{O_2}}+S_{\mathrm{O_2}}} X_H$
3. Anoxic storage on nitrate	$k_{\mathrm{STO}}\eta_{H,\mathrm{NO}x} \frac{S_S}{K_{S,H}+S_S} \frac{K_{H,\mathrm{O_2}}}{K_{H,\mathrm{O_2}}+S_{\mathrm{O_2}}} \frac{S_{\mathrm{NO_3}}}{K_{\mathrm{NO_3}}+S_{\mathrm{NO_3}}} X_H$
4. Anoxic storage on nitrite	$k_{\mathrm{STO}}\eta_{H,\mathrm{NO}x} \frac{S_S}{K_{S,H}+S_S} \frac{K_{H,\mathrm{O_2}}}{K_{H,\mathrm{O_2}}+S_{\mathrm{O_2}}} \frac{S_{NO_2}}{K_{\mathrm{NO_2}}+S_{\mathrm{NO_2}}} X_H$
5. Aerobic growth	$\mu_H \frac{X_{\mathrm{STO}}/X_H}{K_{\mathrm{STO}}+X_{\mathrm{STO}}/X_H} \frac{K_{S,H}}{K_{S,H}+S_S} \frac{S_{\mathrm{O_2}}}{K_{H,\mathrm{O_2}}+S_{\mathrm{O_2}}} \frac{S_{\mathrm{NH_4}}}{K_{H,\mathrm{NH_4}}+S_{\mathrm{NH_4}}} \frac{S_{\mathrm{PO_4}}}{K_{H,\mathrm{PO_4}}+S_{\mathrm{PO_4}}} X_H$
6. Anoxic growth on nitrate	$\mu_H\eta_{H,\mathrm{NO}x} \frac{X_{\mathrm{STO}}/X_H}{K_{\mathrm{STO}}+X_{\mathrm{STO}}/X_H} \frac{K_{S,H}}{K_{S,H}+S_S} \frac{K_{H,\mathrm{O_2}}}{K_{H,\mathrm{O_2}}+S_{\mathrm{O_2}}} \frac{S_{\mathrm{NO_3}}}{K_{\mathrm{NO_3}}+S_{\mathrm{NO_3}}} \frac{S_{\mathrm{NH_4}}}{K_{H,\mathrm{NH_4}}+S_{\mathrm{NH_4}}} \frac{S_{\mathrm{PO_4}}}{K_{H,\mathrm{PO_4}}+S_{\mathrm{PO_4}}} X_H$
7. Anoxic growth on nitrite	$\mu_H\eta_{H,\mathrm{NO}x} \frac{X_{\mathrm{STO}}/X_H}{K_{\mathrm{STO}}+X_{\mathrm{STO}}/X_H} \frac{K_{S,H}}{K_{S,H}+S_S} \frac{K_{H,\mathrm{O_2}}}{K_{H,\mathrm{O_2}}+S_{\mathrm{O_2}}} \frac{S_{\mathrm{NO_2}}}{K_{\mathrm{NO_2}}+S_{\mathrm{NO_2}}} \frac{S_{\mathrm{NH_4}}}{K_{H,\mathrm{NH_4}}+S_{\mathrm{NH_4}}} \frac{S_{\mathrm{PO_4}}}{K_{H,\mathrm{PO_4}}+S_{\mathrm{PO_4}}} X_H$
8. Aerobic endogenous respiration	$b_{H,\mathrm{O_2}} \frac{S_{\mathrm{O_2}}}{K_{H,\mathrm{O_2}}+S_{\mathrm{O_2}}} X_H$
9. Anoxic endogenous respiration	$b_{H,\mathrm{NO}x} \frac{K_{H,\mathrm{O_2}}}{K_{H,\mathrm{O_2}}+S_{\mathrm{O_2}}} \frac{S_{\mathrm{NO_2}}+S_{\mathrm{NO_3}}}{K_{\mathrm{NO}x}+S_{\mathrm{NO_2}}+S_{\mathrm{NO_3}}} X_H$
10. Aerobic respiration of X_{STO}	$b_{\mathrm{STO},\mathrm{O_2}} \frac{S_{\mathrm{O_2}}}{K_{H,\mathrm{O_2}}+S_{\mathrm{O_2}}} X_{\mathrm{STO}}$
11. Anoxic respiration of X_{STO}	$b_{\mathrm{STO},\mathrm{NO}x} \frac{K_{H,\mathrm{O_2}}}{K_{H,\mathrm{O_2}}+S_{\mathrm{O_2}}} \frac{S_{\mathrm{NO_2}}+S_{\mathrm{NO_3}}}{K_{\mathrm{NO}x}+S_{\mathrm{NO_2}}+S_{\mathrm{NO_3}}} X_{\mathrm{STO}}$
Autotrophic organisms	
12. Aerobic growth of X_{AOB}	$\mu_{\mathrm{AOB}} \frac{S_{\mathrm{O_2}}}{K_{A,\mathrm{O_2}}+S_{\mathrm{O_2}}} \frac{S_{\mathrm{NH_4}}}{K_{A,\mathrm{NH_4}}+S_{\mathrm{NH_4}}} \frac{S_{\mathrm{PO_4}}}{K_{A,\mathrm{PO_4}}+S_{\mathrm{PO_4}}} X_{\mathrm{AOB}}$
13. Aerobic growth of X_{NOB}	$\mu_{\mathrm{NOB}} \frac{S_{\mathrm{O_2}}}{K_{A,\mathrm{O_2}}+S_{\mathrm{O_2}}} \frac{K_{I,\mathrm{NH_4}}}{K_{I,\mathrm{NH_4}}+S_{\mathrm{NH_4}}} \frac{S_{\mathrm{NO_2}}}{K_{A,\mathrm{NO_2}}+S_{\mathrm{NO_2}}} \frac{S_{\mathrm{PO_4}}}{K_{A,\mathrm{PO_4}}+S_{\mathrm{PO_4}}} X_{\mathrm{NOB}}$
14. Aerobic endogenous respiration of X_{AOB}	$b_{\mathrm{AOB},\mathrm{O_2}} \frac{S_{\mathrm{O_2}}}{K_{A,\mathrm{O_2}}+S_{\mathrm{O_2}}} X_{\mathrm{AOB}}$
15. Aerobic endogenous respiration of X_{NOB}	$b_{\mathrm{NOB},O_2} \frac{S_{\mathrm{O_2}}}{K_{A,\mathrm{O_2}}+S_{\mathrm{O_2}}} X_{\mathrm{NOB}}$
16. Anoxic endogenous respiration of X_{AOB}	$b_{\mathrm{AOB},\mathrm{NO}x} \frac{K_{A,\mathrm{O_2}}}{K_{A,\mathrm{O_2}}+S_{\mathrm{O_2}}} \frac{S_{\mathrm{NO_2}}+S_{\mathrm{NO_3}}}{K_{\mathrm{NO}x}+S_{\mathrm{NO_2}}+S_{\mathrm{NO_3}}} X_{\mathrm{AOB}}$
17. Anoxic endogenous respiration of X_{NOB}	$b_{\mathrm{NOB},\mathrm{NO}x} \frac{K_{A,\mathrm{O_2}}}{K_{A,\mathrm{O_2}}+S_{\mathrm{O_2}}} \frac{S_{\mathrm{NO_2}}+S_{\mathrm{NO_3}}}{K_{\mathrm{NO}x}+S_{\mathrm{NO_2}}+S_{\mathrm{NO_3}}} X_{\mathrm{NOB}}$
Phosphorus accumulating organisms	
18. Storage of X_{PHA}	$q_{\mathrm{PHA}} \frac{S_S}{K_{S,\mathrm{PAO}}+S_S} \frac{X_{\mathrm{PP}}/X_{\mathrm{PAO}}}{K_{\mathrm{PP,PAO}}+X_{PP}/X_{\mathrm{PAO}}} X_{\mathrm{PAO}}$
19. Aerobic storage of X_{PP}	$q_{\mathrm{PP}} \frac{S_{\mathrm{O_2}}}{K_{\mathrm{PAO},\mathrm{O_2}}+S_{\mathrm{O_2}}} \frac{S_{\mathrm{PO_4}}}{K_{\mathrm{PO_4,PP}}+S_{\mathrm{PO_4}}} \frac{X_{\mathrm{PHA}}/X_{\mathrm{PAO}}}{K_{\mathrm{PHA}}+X_{\mathrm{PHA}}/X_{\mathrm{PAO}}} \frac{K_{\mathrm{max,PAO}}-X_{\mathrm{PP}}/X_{\mathrm{PAO}}}{K_{i\mathrm{PP,PAO}}+K_{\mathrm{max,PAO}}-X_{\mathrm{PP}}/X_{\mathrm{PAO}}} X_{\mathrm{PAO}}$
20. Anoxic storage of X_{PP} on nitrate	$q_{\mathrm{PP}}\eta_{\mathrm{PAO},\mathrm{NO}x} \frac{K_{\mathrm{PAO},\mathrm{O_2}}}{K_{\mathrm{PAO},\mathrm{O_2}}+S_{\mathrm{O_2}}} \frac{S_{\mathrm{NO_3}}}{K_{\mathrm{NO_3}}+S_{\mathrm{NO_3}}} \frac{S_{\mathrm{PO_4}}}{K_{\mathrm{PO_4,PP}}+S_{\mathrm{PO_4}}} \frac{X_{\mathrm{PHA}}/X_{\mathrm{PAO}}}{K_{\mathrm{PHA}}+X_{\mathrm{PHA}}/X_{\mathrm{PAO}}} \frac{K_{\mathrm{max,PAO}}-X_{\mathrm{PP}}/X_{\mathrm{PAO}}}{K_{i\mathrm{PP,PAO}}+K_{\mathrm{max,PAO}}-X_{\mathrm{PP}}/X_{\mathrm{PAO}}} X_{\mathrm{PAO}}$
21. Anoxic storage of X_{PP} on nitrite	$q_{\mathrm{PP}}\eta_{\mathrm{PAO},\mathrm{NO}x} \frac{K_{\mathrm{PAO},\mathrm{O_2}}}{K_{\mathrm{PAO},\mathrm{O_2}}+S_{\mathrm{O_2}}} \frac{S_{\mathrm{NO_2}}}{K_{\mathrm{NO_2}}+S_{\mathrm{NO_2}}} \frac{S_{\mathrm{PO_4}}}{K_{\mathrm{PO_4,PP}}+S_{\mathrm{PO_4}}} \frac{X_{\mathrm{PHA}}/X_{\mathrm{PAO}}}{K_{\mathrm{PHA}}+X_{\mathrm{PHA}}/X_{\mathrm{PAO}}} \frac{K_{\mathrm{max,PAO}}-X_{PP}/X_{\mathrm{PAO}}}{K_{i\mathrm{PP,PAO}}+K_{\mathrm{max,PAO}}-X_{\mathrm{PP}}/X_{\mathrm{PAO}}} X_{\mathrm{PAO}}$
22. Aerobic growth	$\mu_{\mathrm{PAO}} \frac{X_{\mathrm{PHA}}/X_{\mathrm{PAO}}}{K_{\mathrm{PHA}}+X_{\mathrm{PHA}}/X_{\mathrm{PAO}}} \frac{S_{\mathrm{O_2}}}{K_{\mathrm{PAO},\mathrm{O_2}}+S_{\mathrm{O_2}}} \frac{S_{\mathrm{NH_4}}}{K_{\mathrm{PAO},\mathrm{NH_4}}+S_{\mathrm{NH_4}}} \frac{S_{\mathrm{PO_4}}}{K_{\mathrm{PAO},\mathrm{PO_4}}+S_{\mathrm{PO_4}}} X_{\mathrm{PAO}}$
23. Anoxic growth on nitrate	$\mu_{\mathrm{PAO}}\eta_{\mathrm{PAO},\mathrm{NO}x} \frac{X_{\mathrm{PHA}}/X_{\mathrm{PAO}}}{K_{\mathrm{PHA}}+X_{\mathrm{PHA}}/X_{\mathrm{PAO}}} \frac{K_{\mathrm{PAO},\mathrm{O_2}}}{K_{\mathrm{PAO},\mathrm{O_2}}+S_{\mathrm{O_2}}} \frac{S_{\mathrm{NO_3}}}{K_{\mathrm{NO_3}}+S_{\mathrm{NO_3}}} \frac{S_{\mathrm{NH_4}}}{K_{\mathrm{PAO},\mathrm{NH_4}}+S_{\mathrm{NH_4}}} \frac{S_{\mathrm{PO_4}}}{K_{\mathrm{PAO},\mathrm{PO_4}}+S_{\mathrm{PO_4}}} X_{\mathrm{PAO}}$
24. Anoxic growth on nitrite	$\mu_{\mathrm{PAO}}\eta_{\mathrm{PAO},\mathrm{NO}x} \frac{X_{\mathrm{PHA}}/X_{\mathrm{PAO}}}{K_{\mathrm{PHA}}+X_{\mathrm{PHA}}/X_{\mathrm{PAO}}} \frac{K_{\mathrm{PAO},\mathrm{O_2}}}{K_{\mathrm{PAO},\mathrm{O_2}}+S_{\mathrm{O_2}}} \frac{S_{\mathrm{NO_2}}}{K_{\mathrm{NO_2}}+S_{\mathrm{NO_2}}} \frac{S_{\mathrm{NH_4}}}{K_{\mathrm{PAO},\mathrm{NH_4}}+S_{\mathrm{NH_4}}} \frac{S_{\mathrm{PO_4}}}{K_{\mathrm{PAO},\mathrm{PO_4}}+S_{\mathrm{PO_4}}} X_{\mathrm{PAO}}$
25. Aerobic endogenous respiration	$b_{\mathrm{PAO}} \frac{S_{\mathrm{O_2}}}{K_{\mathrm{PAO},\mathrm{O_2}}+S_{\mathrm{O_2}}} X_{\mathrm{PAO}}$
26. Anoxic endogenous respiration	$b_{\mathrm{PAO}}\eta_{\mathrm{PAO},\mathrm{NO}x} \frac{K_{\mathrm{PAO},\mathrm{O_2}}}{K_{\mathrm{PAO},\mathrm{O_2}}+S_{\mathrm{O_2}}} \frac{S_{\mathrm{NO_2}}+S_{\mathrm{NO_3}}}{K_{\mathrm{NO}x}+S_{\mathrm{NO_2}}+S_{\mathrm{NO_3}}} X_{\mathrm{PAO}}$
27. Aerobic respiration of X_{PP}	$b_{\mathrm{PP}} \frac{S_{\mathrm{O_2}}}{K_{\mathrm{PAO},\mathrm{O_2}}+S_{\mathrm{O_2}}} X_{\mathrm{PP}}$
28. Anoxic respiration of X_{PP}	$b_{\mathrm{PP}}\eta_{\mathrm{PAO},\mathrm{NO}x} \frac{K_{\mathrm{PAO},\mathrm{O_2}}}{K_{\mathrm{PAO},\mathrm{O_2}}+S_{\mathrm{O_2}}} \frac{S_{\mathrm{NO_2}}+S_{\mathrm{NO_3}}}{K_{\mathrm{NO}x}+S_{\mathrm{NO_2}}+S_{\mathrm{NO_3}}} X_{\mathrm{PP}}$
29. Aerobic respiration of X_{PHA}	$b_{\mathrm{PHA}} \frac{S_{\mathrm{O_2}}}{K_{\mathrm{PAO},\mathrm{O_2}}+S_{\mathrm{O_2}}} X_{\mathrm{PHA}}$
30. Anoxic respiration of X_{PHA}	$b_{\mathrm{PHA}}\eta_{\mathrm{PAO},\mathrm{NO}x} \frac{K_{\mathrm{PAO},\mathrm{O_2}}}{K_{\mathrm{PAO},\mathrm{O_2}}+S_{\mathrm{O_2}}} \frac{S_{\mathrm{NO_2}}+S_{\mathrm{NO_3}}}{K_{\mathrm{NO}x}+S_{\mathrm{NO_2}}+S_{\mathrm{NO_3}}} X_{\mathrm{PHA}}$

''nitritation'', and nitrite oxidation to nitrate by nitrite oxidizers (NOB), namely ''nitratation''. One limitation of the ASM3 is its simplification of the two-step nitrification process into a single-step reaction. This simplification may cause serious problems in specific applications where nitrite becomes important, either as a target final product or an unwanted intermediate. In our work, the nitrification process is regarded as a two-step reaction, i.e., ammonium oxidation to nitrite and nitrite oxidation to nitrate. The AOB utilize ammonium and the NOB consume nitrite for their aerobic

Table 3. Stoichiometric Matrix for the Heterotrophic Organisms in the Developed Model

Variable Process	S_O	S_S	S_{NH_4}	S_{NO_2}	S_{NO_3}	S_{N_2}	S_{PO_4}	X_H	X_{STO}	X_I
2	$Y_{STO,O_2} - 1$	-1	$i_{N,SS}$				$i_{P,SS}$		Y_{STO,O_2}	
3		-1	$i_{N,SS}$	$\frac{1-Y_{STO,NOx}}{1.14}$	$\frac{Y_{STO,NOx}-1}{1.14}$		$i_{P,SS}$		$Y_{STO,NOx}$	
4		-1	$i_{N,SS}$	$\frac{Y_{STO,NOx}-1}{1.71}$		$\frac{1-Y_{STO,NOx}}{1.71}$	$i_{P,SS}$		$Y_{STO,NOx}$	
5	$\frac{Y_{H,O_2}-1}{Y_{H,O_2}}$		$-i_{N,BM}$				$-i_{P,BM}$	1	$\frac{-1}{Y_{H,O_2}}$	
6			$-i_{N,BM}$	$\frac{1-Y_{H,NOx}}{1.14Y_{H,NOx}}$	$\frac{Y_{H,NOx}-1}{1.14Y_{H,NOx}}$		$-i_{P,BM}$	1	$\frac{-1}{Y_{H,NOx}}$	
7			$-i_{N,BM}$	$\frac{Y_{H,NOx}-1}{1.71Y_{H,NOx}}$		$\frac{1-Y_{H,NOx}}{1.71Y_{H,NOx}}$	$-i_{P,BM}$	1	$\frac{-1}{Y_{H,NOx}}$	
8	$f_I - 1$		$i_{N,BM} - i_{N,XI}f_I$				$i_{P,BM} - i_{P,XI}f_I$	-1		f_I
9			$i_{N,BM} - i_{N,XI}f_I$		$(f_I - 1)/2.86$	$(1 - f_I)/2.86$	$i_{P,BM} - i_{P,XI}f_I$	-1		f_I
10	-1								-1	
11					$-1/2.86$	$1/2.86$			-1	

growth. The growth processes, rate equations and their stoichiometric interactions with the components are shown in Tables 2 and 4 (Processes 12–17).

Phosphorus Accumulating Organisms. In our model, the storage of X_{PHA} (Process 18 in Tables 2 and 5) describes the storage of readily degradable substrate (S_S) in the form of cell-internal storage products (X_{PHA}), according to the EAWAG Bio-P model.[15] The energy that becomes available during the release of polyphosphate (X_{PP}) is used to store the substrate. This process occurs mainly under anaerobic conditions, but is also observed in aerobic and anoxic zones. For this reason, no inhibition terms are implemented in the kinetic expression.

The PAOs require energy for the uptake of orthophosphate (S_{PO4}) and its storage in the form of cell internal polyphosphates (X_{PP}). This energy can be obtained from the aerobic or anoxic respiration of X_{PHA}. An inhibition term is implemented to take a maximum P-content of the PAOs into account. To account for the reduced P uptake under anoxic conditions, a separate kinetics for P uptake per PHA utilized is introduced for anoxic conditions (Processes 20 and 21 in Table 5). In the two anoxic P uptake processes, nitrate (Process 20) or nitrite (Process 21) is respired instead of oxygen. A reduction factor ($\eta_{PAO,NOx}$) is introduced because not all PAOs are capable of denitrification, which may only proceed at a reduced rate, compared with the aerobic P uptake.

In the EAWAG Bio-P and ASM 2/2d models, PAOs grow only on the stored PHA. For this growth, the aerobic growth process of PAOs present in the EAWAG Bio-P model is included without modification (Process 22 in Tables 2 and 5). Additionally, two anoxic processes are included for the anoxic PAOs growth on PHA under denitrifying conditions. In this case, PAOs can utilize PHA for their synthesis through anoxic respiration on either nitrite or nitrate, which serves as an electron acceptor instead of using DO (Processes 23 and 24 in Tables 2 and 5). To accommodate anoxic growth of PAOs, their aerobic growth processes (Process 22 in Tables 2 and 5) are duplicated for anoxic conditions (Processes 23 and 24 in Tables 2 and 5), but with the processes rates multiplied by the reduction factor $\eta_{PAO,NOx}$. In addition, a separate anoxic growth yield coefficient for PAOs ($Y_{PAO,NOx}$, see Table 5) is introduced into the model. The aerobic yield coefficient is reduced by a ratio to give an anoxic yield coefficient.

Aerobic (Process 25 in Tables 2 and 5) and anoxic (Process 26 in Tables 2 and 5) endogenous respiration processes of PAOs account for all forms of biomass loss and energy requirements not associated with growth by considering the related respiration under both aerobic and anoxic conditions, including decay, endogenous respiration, lysis, predation, motility, death, etc. The anoxic endogenous respiration is similar to the aerobic process, but both nitrite and nitrate, instead of DO, serve as an electron acceptor, and the reduction factor $\eta_{PAO,NOx}$ should be introduced. Aerobic (Processes 27 and 29 in Tables 2 and 5) and anoxic (Processes 28 and 30 in Tables 2 and 5) respiration and lysis of the internal storage products (X_{PP} and X_{PHA}) processes are analogous to the endogenous respiration of the biomass, which ensures that the storage products decay along with the biomass.

Stoichiometry and kinetics

The stoichiometric matrix for our model is shown in Tables 3–5, whereas all stoichiometric parameters are

Table 4. Stoichiometric Matrix for the Autotrophic Organisms in the Developed Model

Variable Process	S_O	S_{NH_4}	S_{NO_2}	S_{NO_3}	S_{N_2}	S_{PO_4}	X_{AOB}	X_{NOB}	X_I
12	$\frac{Y_{AOB}-3.43}{Y_{AOB}}$	$-\frac{1}{Y_{AOB}} - i_{N,BM}$	$1/Y_{AOB}$			$-i_{P,BM}$	1		
13	$\frac{Y_{NOB}-1.14}{Y_{NOB}}$	$-i_{N,BM}$	$-1/Y_{NOB}$	$1/Y_{NOB}$		$-i_{P,BM}$		1	
14	$f_I - 1$	$i_{N,BM} - i_{N,XI}f_I$				$i_{P,BM} - i_{P,XI}f_I$	-1		f_I
15	$f_I - 1$	$i_{N,BM} - i_{N,XI}f_I$				$i_{P,BM} - i_{P,XI}f_I$		-1	f_I
16		$i_{N,BM} - i_{N,XI}f_I$		$(f_I - 1)/2.86$	$(1 - f_I)/2.86$	$i_{P,BM} - i_{P,XI}f_I$	-1		f_I
17		$i_{N,BM} - i_{N,XI}f_I$		$(f_I - 1)/2.86$	$(1 - f_I)/2.86$	$i_{P,BM} - i_{P,XI}f_I$		-1	f_I

Table 5. Stoichiometric Matrix for the Phosphorus Accumulating Organisms in the Developed Model

Variable Process	S_O	S_S	S_{NH_4}	S_{NO_2}	S_{NO_3}	S_{N_2}	S_{PO_4}	X_{PAO}	X_{PP}	X_{PHA}	X_I
18		-1	$i_{N,SS}$				$Y_{PO_4}+i_{P,SS}$		$-Y_{PO_4}$	1	
19	$-Y_{PHA}$						-1		1	$-Y_{PHA}$	
20				$Y_{PHA}/1.14$	$-Y_{PHA}/1.14$		-1		1	$-Y_{PHA}$	
21				$-Y_{PHA}/1.71$		$Y_{PHA}/1.71$	-1		1	$-Y_{PHA}$	
22	$\frac{Y_{PAO,O_2}-1}{Y_{PAO,O_2}}$		$-i_{N,BM}$				$-i_{P,BM}$	1		$\frac{-1}{Y_{PAO,O_2}}$	
23			$-i_{N,BM}$	$\frac{1-Y_{PAO,NOx}}{1.14Y_{PAO,NOx}}$	$\frac{Y_{PAO,NOx}-1}{1.14Y_{PAO,NOx}}$		$-i_{P,BM}$	1		$\frac{-1}{Y_{PAO,NOx}}$	
24			$-i_{N,BM}$	$\frac{Y_{PAO,NOx}-1}{1.71Y_{PAO,NOx}}$		$\frac{1-Y_{PAO,NOx}}{1.71Y_{PAO,NOx}}$	$-i_{P,BM}$	1		$\frac{-1}{Y_{PAO,NOx}}$	
25	f_I-1		$i_{N,BM}-i_{N,XI}f_I$				$i_{P,BM}-i_{P,XI}f_I$	-1			f_I
26			$i_{N,BM}-i_{N,XI}f_I$		$(f_I-1)/2.86$	$(1-f_I)/2.86$	$i_{P,BM}-i_{P,XI}f_I$	-1			f_I
27							1		-1		
28							1		-1		
29	-1									-1	
30					$-1/2.86$	$1/2.86$				-1	

explained and listed in Table 6. The distinct aerobic and anoxic yields are applied in our model, which is a modification to ASM3. Furthermore, nitrification process has been extended into two steps as described earlier: nitritation and nitratation. Thus, two separated yield coefficients are included. Y_{AOB} and Y_{NOB} are the yield coefficients of AOB and NOB, respectively. When one unit of S_{NH4} or S_{NO_2} is utilized for AOB or NOB growth, a stoichiometric ratio of $(3.43-Y_{NH_4})$ or $(1.14-Y_{NO_2})$ is applicable for the amount of dissolve oxygen (S_O) consumed in the two-step nitrification process.

Table 2 shows the kinetics of the developed model. The kinetic parameters are listed in Table 6 with their definitions and units. Similarly, the kinetic rate equations have been modified significantly through the inclusion of the two-step nitrification–denitrification, the anoxic P uptake, and the two-step denitrification by PAOs (Table 2). For instance, μ_{AOB} and μ_{NOB} are the two different maximum specific growth rate constants for the AOB (X_{AOB}) and NOB (X_{NOB}) groups, respectively, with K_{NH4} and K_{NO2} are the half-saturation constants for the growth of the related microbial groups.

Definitions and default values for all the kinetic and stoichiometric coefficients of our model are shown in Table 6. The sources for the default values of all the parameters are also included. The calibration of the parameters is presented subsequently.

Materials and Methods

Description of the full-scale WWTP for BNR

A full-scale WWTP, consisted of primary clarifiers and four lines of the activated sludge systems, is an A/A/O (Anaerobic-Anoxic-Aerobic) process as shown in Figure 1. This plant was designed for removal of COD, N and P from domestic and industrial wastewaters of nearby communities. After primary sedimentation, wastewater is introduced into the activated sludge units in parallel, each consisting of three concentric compartments, i.e., anaerobic tank, anoxic tank, and aerobic tank. With diffused aeration, agitation by propellers and a high internal recirculation, the activated sludge in these units is well mixed. The activated sludge leaves the aerobic tank via a weir prior to splitting into secondary settlers. After settling, the purified sewage is discharged into a river. A large fraction of the settled activated sludge (secondary sludge) is returned to the anaerobic tank to maintain the desired biomass content, whereas the remaining part (excess sludge) is wasted. The mixed liquor recirculation and returned activated sludge recirculation are usually set at 300% of influent flux and 80% of influent flux, respectively.

The reactor volumes of the anaerobic, anoxic, and aerobic tanks are 3,220, 6,441, and 22,543 m^3, respectively. Their corresponding hydraulic retention times are 1.5, 3.2, and 10.8 h, respectively, with an influent flow rate of 2150 m^3 h^{-1}. The operating sludge retention time of the Anaerobic-Anoxic-Aerobic activated sludge system is ~10 days. The constituent characteristics of the influent and the effluent are listed in Table 7.

Experimental data collection

The recordings of routine measurements for this full-scale WWTP are used as a data source for dynamic simulation. The measurements include COD, ammonia (NH_4^+—N), nitrate (NO_3^-—N), nitrite (NO_2^-), phosphate (PO_4^{3-}—P), mixed liquid suspended solid (MLSS), and mixed liquid volatile suspended solid concentrations. These measurements were conducted according to the Standard Methods.[27]

Influent characterization

The active and endogenous biomass concentrations of the ordinary heterotrophic organisms (X_H), ammonia-oxidizing organisms (X_{AOB}), nitrite-oxidizing organisms (X_{NOB}), and polyphosphate accumulating organisms (X_{PAO}) are experimentally determined following the methods of Wentzel et al.[28] The biodegradable COD (BCOD) in the influent was the sum of the readily biodegradable soluble COD (S_S) and the slowly biodegradable particulate COD (X_S).[29] The biodegradable COD (BCOD and S_S+X_S) concentration was calculated according to Grady et al.[8] The inert fraction S_I was determined independently and subtracted from the soluble COD to give the fraction S_S. S_I was evaluated from the inert COD in the effluent of the WWTP. The concentrations of X_S

Table 6. Definition and Default Values for the Kinetic and Stoichiometric Coefficients in the Developed Model

Symbol	Definition	Values	Unit	Source
Composition factors				
$i_{N,BM}$	Nitrogen content of biomass	0.07	g N g^{-1} COD	(a)
$i_{P,BM}$	Phosphorus content of biomass	0.02	g P g^{-1} COD	(a)
$i_{N,XI}$	Nitrogen content of X_I	0.02	g N g^{-1} COD	(a)
$i_{P,XI}$	Phosphorus content of X_I	0.01	g P g^{-1} COD	(a)
$i_{N,SS}$	Nitrogen content of S_S	0.03	g N g^{-1} COD	(a)
$i_{P,SS}$	Phosphorus content of S_S	0.01	g P g^{-1} COD	(a)
Hydrolysis				
k_H	Hydrolysis rate constant	0.125	h^{-1}	(b)
K_X	Hydrolysis saturation constant	1.0	g COD g^{-1} COD	(b)
Heterotrophic organisms				
Y_{STO,O_2}	Aerobic yield coefficient for X_H storage	0.85	g COD g^{-1} COD	(b)
$Y_{STO,NOx}$	Anoxic yield coefficient for X_H storage	0.80	g COD g^{-1} COD	(b)
Y_{H,O_2}	Aerobic yield coefficient for X_H growth	0.63	g COD g^{-1} COD	(b)
$Y_{H,NOx}$	Anoxic yield coefficient for X_H growth	0.54	g COD g^{-1} COD	(b)
$\eta_{H,NOx}$	Anoxic reduction factor	0.6	—	(b)
f_I	Fraction of X_I in endogenous respiration	0.2	g COD g^{-1} COD	(b)
k_{STO}	Storage rate constant of X_H on S_S	0.21	h^{-1}	(b)
μ_H	Maximum growth rate of X_H on X_{STO}	0.083	h^{-1}	(b)
b_{H,O_2}	Aerobic respiration rate of X_H	0.0083	h^{-1}	(b)
$b_{H,NOx}$	Anoxic respiration rate of X_H	0.0042	h^{-1}	(b)
b_{STO,O_2}	Aerobic respiration rate of X_{STO}	0.0083	h^{-1}	(b)
$b_{STO,NOx}$	Anoxic respiration rate of X_{STO}	0.0042	h^{-1}	(b)
$K_{S,H}$	Biomass affinity constant of X_H for S_S	2.0	g COD m^{-3}	(b)
K_{STO}	Biomass affinity constant of X_H for X_{STO}	1.0	g COD g^{-1} COD	(b)
K_{H,O_2}	Dissolve oxygen affinity constant of X_H	0.20	g O_2 m^{-3}	(b)
K_{H,NH_4}	Ammonia affinity constant of X_H	0.01	g N m^{-3}	(b)
K_{H,PO_4}	Phosphorus affinity constant of X_H	0.01	g P m^{-3}	(a)
K_{NO_3}	Biomass nitrate affinity constant	0.50	g N m^{-3}	(b)
K_{NO_2}	Biomass nitrite affinity constant	0.50	g N m^{-3}	(b)
K_{NOx}	Biomass S_{NOx} affinity constant	0.50	g N m^{-3}	(b)
Autotrophic organisms				
Y_{AOB}	Yield coefficient for X_{AOB} growth	0.15	g COD g^{-1} N	(c)
Y_{NOB}	Yield coefficient for X_{NOB} growth	0.041	g COD g^{-1} N	(c)
f_I	Fraction of X_I in endogenous respiration	0.2	g COD g^{-1} COD	(b)
μ_{AOB}	Maximum growth rate of X_{AOB}	0.017	h^{-1}	(c)
μ_{NOB}	Maximum growth rate of X_{NOB}	0.046	h^{-1}	(c)
b_{AOB,O_2}	Aerobic respiration rate of X_{AOB}	0.0042	h^{-1}	(c)
$b_{AOB,NOx}$	Anoxic respiration rate of X_{AOB}	0.0013	h^{-1}	(c)
b_{NOB,O_2}	Aerobic respiration rate of X_{NOB}	0.0025	h^{-1}	(c)
$b_{NOB,NOx}$	Anoxic respiration rate of X_{NOB}	0.0013	h^{-1}	(c)
K_{A,O_2}	Autotrophic oxygen affinity constant	0.5	g O_2 m^{-3}	(b)
K_{A,NH_4}	Ammonia affinity constant of X_{AOB}	2.4	g N m^{-3}	(c)
K_{A,NO_2}	Nitrite affinity constant of X_{NOB}	0.238	g N m^{-3}	(c)
K_{A,PO_4}	Autotrophic S_{PO_4} affinity constant	0.01	g P m^{-3}	(a)
K_{I,NH_4}	Ammonia inhibition of nitrite oxidation	5.0	g N m^{-3}	(d)
K_{NOx}	Biomass S_{NOx} affinity constant	0.50	g N m^{-3}	(b)
Phosphorus accumulating organisms				
Y_{PO_4}	Requirement of X_{PP} per X_{PHA} storage	0.35	g P g^{-1} COD	(e)
Y_{PHA}	Requirement of X_{PHA} per X_{PP} storage	0.2	g COD g^{-1} P	(e)
Y_{PAO,O_2}	Aerobic yield coefficient for X_{PAO}	0.6	g COD g^{-1} COD	(e)
$Y_{PAO,NOx}$	Anoxic yield coefficient for X_{PAO}	0.5	g COD g^{-1} COD	(e)
f_I	Fraction of X_I in endogenous respiration	0.2	g COD g^{-1} COD	(e)
$\eta_{PAO,NOx}$	Anoxic reduction factor	0.6	—	(a)
q_{PHA}	Rate constant for storage of X_{PHA}	0.25	h^{-1}	(e)
q_{PP}	Rate constant for storage of X_{PP}	0.0625	h^{-1}	(e)
μ_{PAO}	Maximum growth rate of X_{PAO}	0.0417	h^{-1}	(e)
b_{PAO}	Endogenous respiration rate of X_{PAO}	0.0083	h^{-1}	(e)
b_{PP}	Lysis of X_{PP}	0.0083	h^{-1}	(e)
b_{PHA}	Respiration rate for X_{PHA}	0.0083	h^{-1}	(e)
$K_{S,PAO}$	Biomass saturation constant for S_S	10	g COD m^{-3}	(e)
$K_{PP,PAO}$	Saturation constant for X_{PP}/X_{PAO}	0.05	g P g^{-1} COD	(e)
K_{PAO,O_2}	Biomass saturation constant for S_O	0.2	g O_2 m^{-3}	(e)
$K_{PO_4,PP}$	Saturation constant for S_{PO_4} of storage	0.2	g P m^{-3}	(e)
K_{PHA}	Saturation constant for X_{PHA}/X_{PAO}	0.1	g COD g^{-1} COD	(e)
$K_{iPP,PAO}$	Saturation for $K_{max,PAO}$-(X_{PP}/X_{PAO})	0.05	g P g^{-1} COD	(e)
$K_{max,PAO}$	Maximum ratio of X_{PP}/X_{PAO}	0.2	g P g^{-1} COD	(e)
K_{PAO,NH_4}	Biomass saturation constant for S_{NH_4}	0.01	g N g^{-1} m^{-3}	(e)
K_{PAO,PO_4}	Saturation constant for S_{PO_4} of growth	0.05	g P g^{-1} m^{-3}	(e)
K_{NO_3}	Biomass nitrate affinity constant	0.50	g N m^{-3}	(e)
K_{NO_2}	Biomass nitrite affinity constant	0.50	g N m^{-3}	(e)
K_{NOx}	Biomass S_{NOx} affinity constant	0.50	g N m^{-3}	(e)

(a) Henze et al.[20]; (b) Gujer et al.[14]; (c) de Kreuk et al.[5]; (d) Henze et al.[12]; (e) Rieger et al.[15]

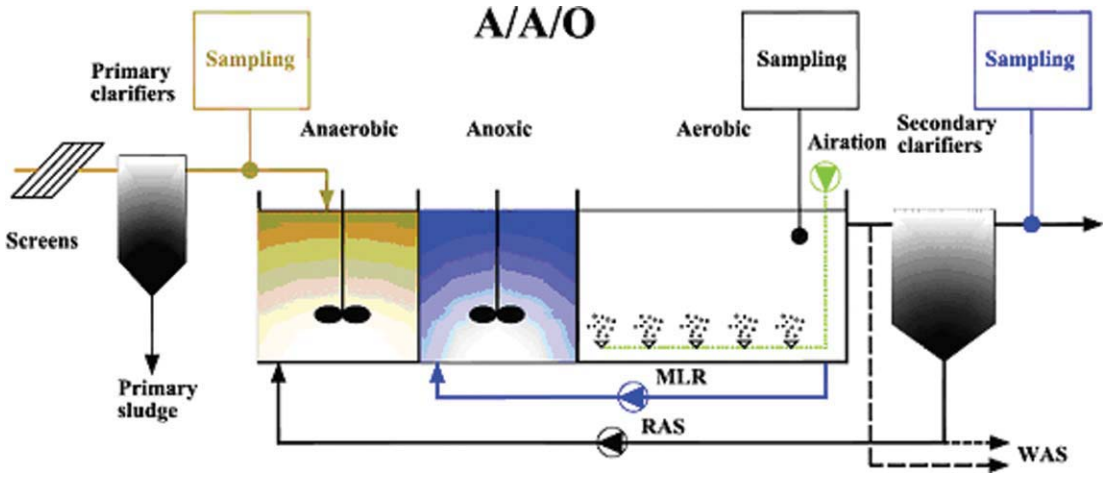

Figure 1. A flow sheet of the A/A/O process at the full-scale WWTP.

[Color figure can be viewed in the online issue, which is available at www.interscience.wiley.com.]

and X_I were estimated based on the BOD_5 measurements.[30] With the characterization of the organic fractions S_I, S_S and X_S, the fraction X_I could be found to be the difference between the total COD and the other fractions. The fractionation was performed on each consecutive day during the long-term simulation period.

Simulation approach

In this work all simulation and parameter estimation were performed with a nonlinear least-squares algorithm in the AQUASIM software package.[31] This program offers a free definition of the biokinetic model, flow scheme, and process control strategies, graphic support of the simulation, experimental data, and communication with spreadsheet programs.[6]

Results and Discussion

Influent characterization

For the influent wastewater of the WWTP, the active and endogenous biomass concentrations of the ordinary heterotrophic organisms (X_H), ammonia-oxidizing organisms (X_{AOB}), nitrite-oxidizing organisms (X_{NOB}), and polyphosphate accumulating organisms (X_{PAO}) are experimentally determined and all of them are found to be close to zero. Thus, the total influent COD can be simply characterized as the sum of S_S, X_S, S_I, and X_I. The average contribution of the individual model components, i.e., S_S, X_S, S_I, and X_I, to the total influent COD is calculated prior to model calibration. During the simulation period, the influent COD fraction did not fluctuate substantially. The S_S fraction is measured to be ~23% of the total COD after settling, and this value is comparable with the results of other studies[4,9,30] in which the S_S concentration of the settled wastewater constitutes 26–32% of the total COD. The initially S_I fraction is estimated to be ~6% of the total COD. The initially established X_I fraction, 22% of the total COD, lies within the range of 10–29% reported in the literature.[4,9,10,30,32] The contribution of X_S is calculated to be 49% of the total COD. Thus, the $S_S/(S_S + X_S)$ ratio is calculated and the values remain within the suggested range of 0.3–0.5.[9]

Model calibration

Model calibration procedure is a process of adjusting coefficient values of the model, so that the results produced by the model with these coefficients closely match the measured data. Our model incorporates a number of stoichiometric and kinetic parameters relating to X_H, X_{AOB}, X_{NOB}, and X_{PAO}. With regard to the stoichiometric and kinetic parameters, most of these values are taken from the previous studies to reduce the number of parameters to be calibrated.[5,12–15] However, with the modifications through the introduction of two-step nitrification–denitrification, anoxic P uptake, and two-step denitrification by PAOs, a number of associated new stoichiometric and kinetic parameters are introduced into in our model. They include: yield coefficient for X_{AOB} growth (Y_{AOB}), yield coefficient for X_{NOB} growth (Y_{NOB}), maximum growth rate of X_{AOB} (μ_{AOB}), maximum growth rate of X_{NOB} (μ_{NOB}), ammonia inhibition of nitrite oxidation ($K_{I,NH4}$), anoxic yield coefficient for X_{PAO} ($Y_{PAO,NOx}$), anoxic reduction factor of X_H ($\eta_{H,NOx}$), and anoxic reduction factor of PAOs ($\eta_{PAO,NOx}$), etc.

The parameter values are estimated by minimizing the sum of squares of the deviations between the measured data and the model predictions with the objective function given as below:

$$F(p) = \left(\sum_{i=1}^{n} \left(y_{\exp,i} - y(p)_i \right)^2 \right)^{1/2} \quad (1)$$

where y_{exp} and $y(p)$ are vectors of n measured values and model predictions at times t_i (i from 1 to n), and p is the

Table 7. Characteristics of the Influent and Effluent for the Full-scale WWTP (The Standard Deviations are Listed in Parentheses just After the Average Values)

Characteristics	Influent	Effluent
COD (mg L^{-1})	400 (100)	35 (10)
BOD_5 (mg L^{-1})	200 (50)	4.0 (3.0)
NH_4^+—N (mg L^{-1})	45 (15)	5.0 (10)
NO_2^-—N (mg L^{-1})	0.1 (0.1)	2.5 (3.0)
NO_3^-—N (mg L^{-1})	0.5 (0.5)	6.0 (7.0)
PO_4^{-}—P (mg L^{-1})	5.0 (4.0)	1.0 (1.5)

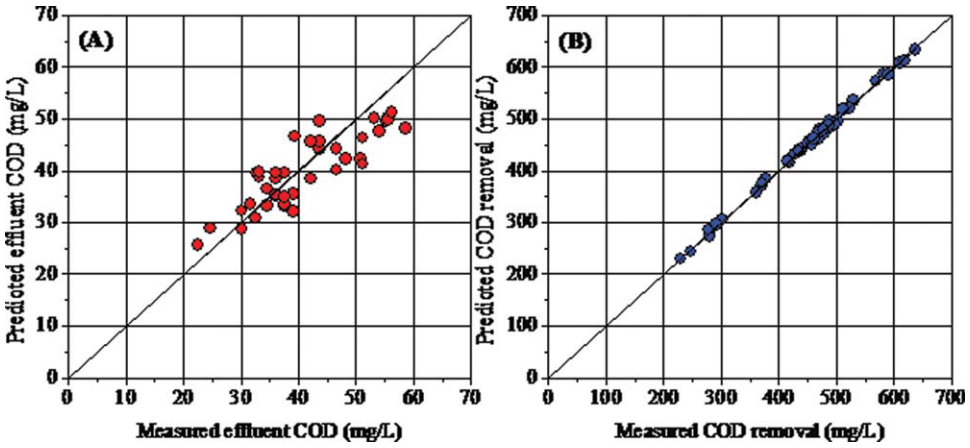

Figure 2. Measured and predicted results of the full-scale WWTP in model calibrations: (A) effluent COD concentrations and (B) COD removal contents.

[Color figure can be viewed in the online issue, which is available at www.interscience.wiley.com.]

vector of the model parameters. The standard deviation in parameter determination is required to be lower than 50% to ensure the validity of the values of the obtained parameters. The identifiability of the model is investigated by starting the minimizing of the objective function (Eq. 1) with different initial conditions on the parameters and examining if the results (the values of the optimal parameters) are consistent or not. The approach used in our work is to change the studied parameters with a certain percentage of their nominal and the behavior of the model

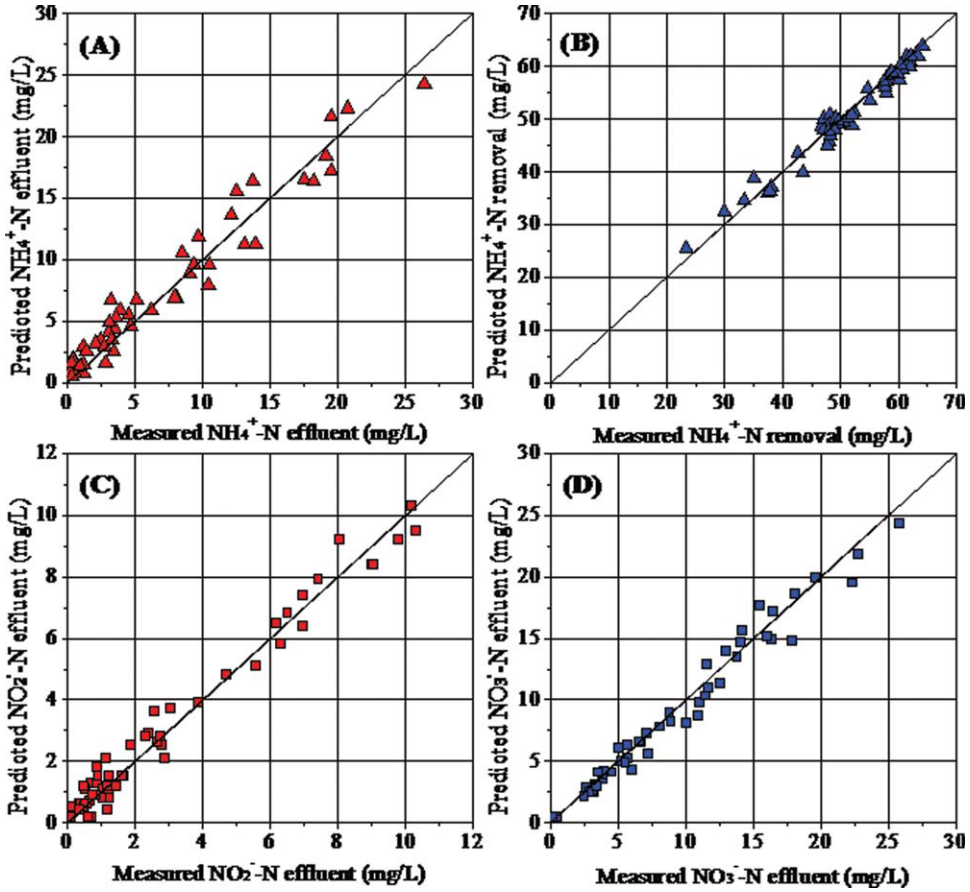

Figure 3. Measured and predicted results of the full-scale WWTP in model calibrations: (A) effluent ammonia concentrations; (B) ammonia removal contents; (C) effluent nitrite concentrations; and (D) effluent nitrate concentrations.

[Color figure can be viewed in the online issue, which is available at www.interscience.wiley.com.]

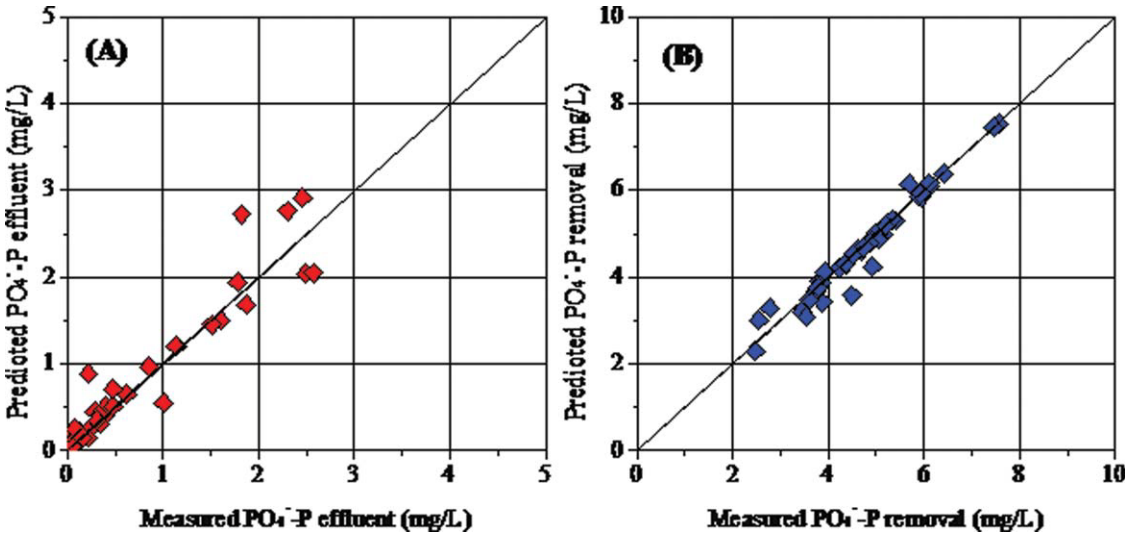

Figure 4. Measured and predicted results of the full-scale WWTP in model calibrations: (A) effluent PO_4^{3-}—P concentrations; and (B) PO_4^{3-}—P removal contents.

[Color figure can be viewed in the online issue, which is available at www.interscience.wiley.com.]

is evaluated as a consequence of a variation of the input parameters.

The values for Y_{AOB}, Y_{NOB}, and $Y_{PAO,NOx}$ are obtained from the experimental data reported in the literature,[5,15] but the values for $\eta_{H,NOx}$ and $\eta_{PAO,NOx}$ should be estimated through fitting simulation results to the experimental data.[33,34] To find appropriate values for $\eta_{H,NOx}$ and $\eta_{PAO,NOx}$ for the full-scale BNR WWTP, the values for $\eta_{H,NOx}$ and $\eta_{PAO,NOx}$ are adjusted until the predicted effluent nitrate and nitrite concentrations match those measured. The parameters of μ_{AOB} and μ_{NOB} for the two nitrifiers (AOB and NOB) are usually considered to be wastewater characteristics-dependent,[33–35] because they vary from system to system and are significantly influenced by the wastewater characteristics. Accordingly, their actual values have to be calibrated for each system by simulation, until the predicted effluent ammonia matches the measured. In addition, our model is also calibrated with the experimentally determined COD removal through adjusting the storage rate constant of X_H on S_S (k_{STO}) and maximum growth rate of X_H on X_{STO} (μ_H). Similarly, the experimentally determined P uptake is used to calibrate the rate constant for storage of X_{PP} (q_{PP}) and maximum growth rate of X_{PAO} (μ_{PAO}). The model calibration processes are described in detail in the subsequent subsections.

COD Consumption. For the simulated WWTP, the COD removal content is first evaluated for model calibration. It should be noted that the substrate type, reactor operating conditions, and microbial communities are important factors affecting the organic substrate consumption processes. Thus, the substrate-consumption-related kinetic parameters, i.e., k_{STO} and μ_H, should be calibrated for different WWTPs.[36] The predicted effluent COD concentrations and COD removal contents match the measured results well after adjusting the two parameters (Figure 2). After calibration, a k_{STO} value of 0.14 h^{-1} and a μ_H value of 0.12 h^{-1} can be applied to this BNR WWTP. The obtained optimal k_{STO} and μ_H values are consistent at different initial values of the parameters, indicating the identifiability of the model.

Two-Step Nitrification–Denitrification. In our model, the two-step nitrification–denitrification processes are included to better model the N conversion dynamics of. The model simulations are evaluated by comparing the predicted results with the measured. The parameters of μ_{AOB} and μ_{NOB} for the two nitrifiers (AOB and NOB) and the two anoxic reduction factors of $\eta_{H,NOx}$ (for X_H) and $\eta_{PAO,NOx}$ (for X_{PAO}) are adjusted until the simulated effluent ammonia, nitrite, and nitrate concentrations and ammonia removal contents closely match the measured results. The values μ_{AOB} and μ_{NOB} are calibrated to be 0.028 h^{-1} and 0.039 h^{-1}, respectively. The parameters of $\eta_{H,NOx}$ and $\eta_{PAO,NOx}$ are determined to be 0.48 and 0.52, giving a good fit with the predicted two-step nitrification–denitrification behavior. The calibrated kinetic parameter values in this work are comparable with those reported in the literature.[3,5,7,14,15,20,30,32,37] Furthermore, these calibrated kinetic parameter values are consistent at different initial values of the parameters. Thus, the model has a good identifiability. As shown in Figure 3, the calibrated model gives good predictions for this full-scale WWTP.

Biological P Uptake. The comparison between the predicted PO_4^{3-}—P removal contents and the effluent PO_4^{3-}—P concentrations with the measured results is shown in Figure 4, and a good agreement between the predictions and the measurements is observed. In the model simulation, the kinetic parameters of P uptake (q_{PP} and μ_{PAO}) have a significant effect on the predictions for biological P uptake in the full-scale WWTP. To improve the simulations for this BNR system, a value of 0.105 h^{-1} for q_{PP} and a value of 0.058 h^{-1} for μ_{PAO} are obtained after model calibration with the experimental results. Also, the calibrated value of q_{PP} and μ_{PAO} are consistent at different initial values, suggesting the identifiability of the model again.

Model validation

Model validation was based on the comparison between the model predictions from the calibrated parameters in the

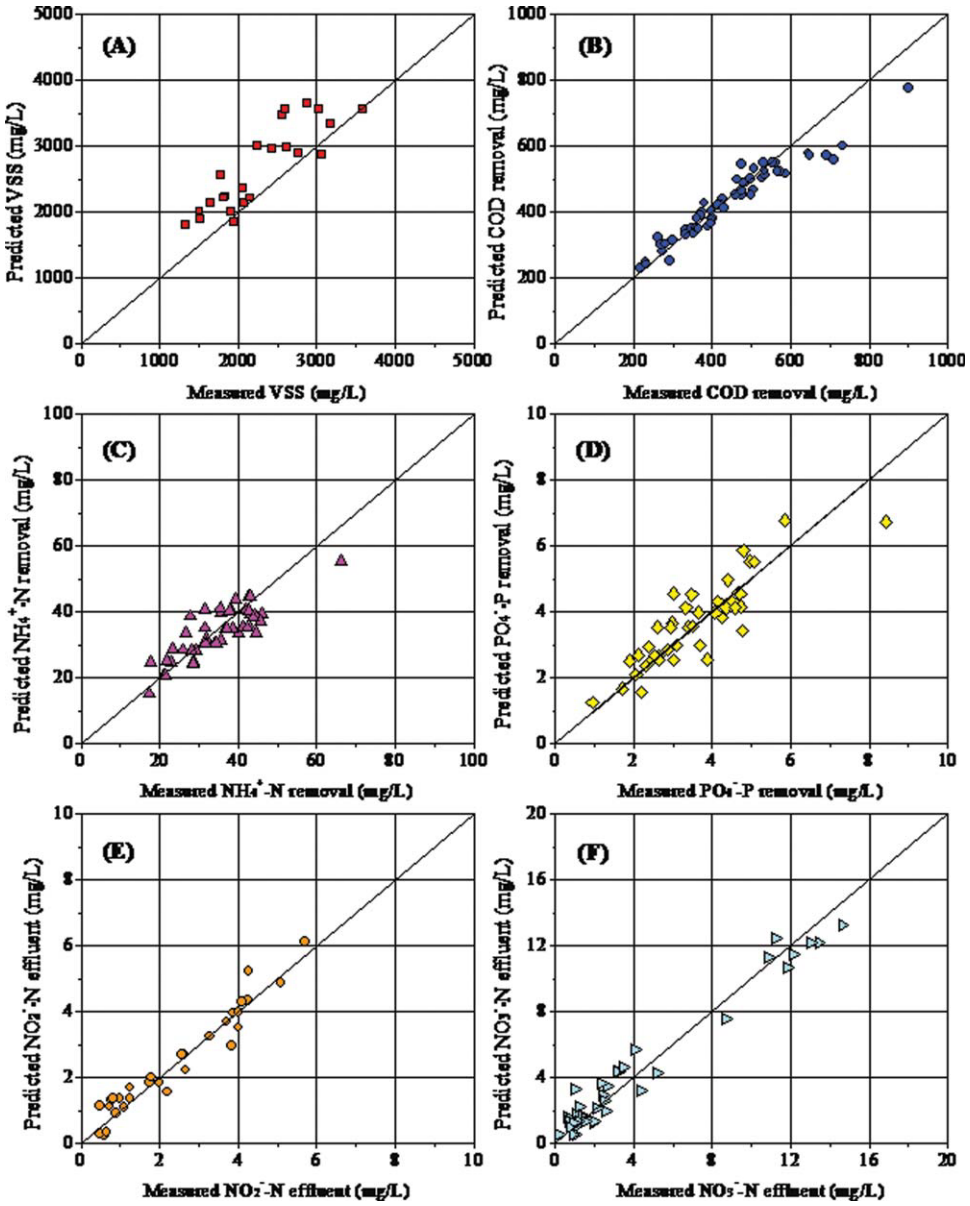

Figure 5. Measured and predicted results of the full-scale WWTP in model validations: (A) VSS concentrations; (B) COD removal contents; (C) ammonia removal contents; (D) PO_4^{3-}—P removal contents; (E) effluent nitrite concentrations; and (F) effluent nitrate concentrations.

[Color figure can be viewed in the online issue, which is available at www.interscience.wiley.com.]

section earlier (no parameters were changed in the subsequent validation step) and the experimental data, which were not used in the calibrations earlier. The validation results are shown in Figure 5. The model results match the trends in biomass production (i.e., MLVSS concentrations), COD consumption, ammonia removal, effluent nitrite and nitrate concentrations, and biological P uptake for the full-scale WWTP. The maximum difference between the measured and calculated values is 20%, and 70% of the results have a difference by less than 10%. Furthermore, the model shows no systematic deviations.

The predicted VSS concentrations in the aerobic tank versus are shown in Figure 5A with the measured results. The model gives reasonable VSS predictions. However, the predicted VSS concentrations are higher than the measured ones in most case. Such a discrepancy may be attributed to the estimated higher fractions for the influent COD concentration, which is non-biodegradable particulate in the influent characterization. As shown in Figure 5B, the predicted COD show a close correlation with the measured one, suggesting that the calibrated parameters can be applicable in this full-scale WWTP.

It is noted that the predicted ammonia removals are slightly higher than the measured values in some cases (Figure 5C). This is associated with the fact that denitrification may partially take place in the aerobic tank because of an air supply shortage problem.[34] The both predicted and measured P uptake efficiencies are shown in Figure 5D and

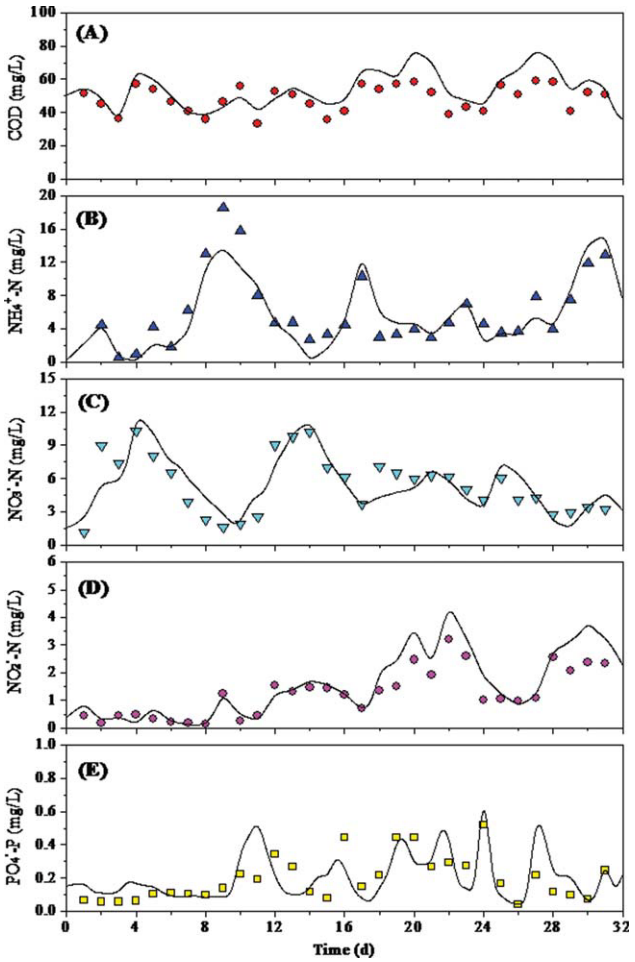

Figure 6. Measured (points) and predicted (lines) results of the full-scale WWTP in its 1-month operation: (A) effluent COD; (B) effluent ammonia; (C) effluent nitrite; (D) effluent nitrate; and (E) effluent PO_4^{3-}—P

[Color figure can be viewed in the online issue, which is available at www.interscience.wiley.com.]

a close correlation is observed. This supports for the inclusion of denitrifying PAOs, two-step PAO denitrification, and anoxic P uptake into our model, and also demonstrates the effectiveness of the calibrated values for the processes. For denitrification, the model gives reasonable simulation results for the effluent nitrite and nitrate concentrations (Figures 5E, F). Because of the inclusion of the two-step nitrification–denitrification into our model, the predicted effluent nitrite concentrations match the measured ones. Thus, with the calibrated parameters, the developed model is applicable to simulate this full-scale WWTP.

Long-term simulation

Over 1-month operating data of this WWTP, which are not previously used for model calibration, are employed for model evaluation. The selected simulation results are illustrated in Figure 6 along with the measured data. There is a close correlation between the measured and the modeled results. The predicted effluent COD levels match the measured ones. Moreover, the model is capable of accurately simulating the short-term effects resulting from the variation of influent COD loading in which high simulated peaks of COD are observed at the high influent COD levels (Figure 6A).

A good prediction is also observed with respect to the effluent NH_4^+-N concentration and its disturbance (Figure 6B). The mean value of the differences between the measured data and model predictions is relatively low. For the long-term dynamic behavior of nitrite and nitrate, the average difference between the simulated and measured effluent nitrite (Figure 6C) and nitrate concentrations (Figure 6D) is less than 2 mg N L^{-1}, showing a good agreement. Regarding the effluent PO_4^{3-}—P concentrations, the model is also capable of simulating the disturbances under hydraulic stress conditions (Figure 6E). The difference between the simulated and measured PO_4^{3-}—P concentrations is $\sim$ 15%. Even though such a value appears to be high, the model is able to reasonably predict the PO_4^{3-}—P changing trends (Figure 6E).

Conclusions

In this work a mechanistic model is developed and used to simulate and predict the operating performance of activated sludge BNR systems for municipal wastewater treatment. Such a model is based on the ASM3 and the EAWAG Bio-P model with significant modifications, e.g., inclusion of the two-step nitrification–denitrification, the anoxic P uptake, and the associated two-step denitrification by PAOs. After incorporating all these processes and characterizing the influent wastewater, the model is capable of simulating and predicting the full-scale BNR WWTP in terms of COD and ammonia removal, effluent nitrite and nitrate concentrations, biological P uptake, and biomass production. Moreover, the model is able to accurately simulate the 1-month continuous operating performance and the short-term effects resulting from the variation of influent loading. The prerequisite for a successful application of this model is the implementation of an extensive calibration and validation procedure, as demonstrated in this work. Such a modeling exercise is not only carried out to gain more experience from practical application of the model, but is also beneficial to a better understanding of plant operation and treatment processes and to a further optimization of WWTPs.

Acknowledgments

The authors wish to thank the Natural Science Foundation of China (50625825 and 50738006), and the Key Special Program on the S&T for the Pollution Control and Treatment of Water Bodies (2008ZX07316-002 and 2008ZX07010-005) for the partial support of this study.

Literature Cited

1. Smolders GJF, van der Meij J, van Loosdrecht MCM, Heijnen JJ. A structured metabolic model for the anaerobic and aerobic stoichiometry and kinetics of the biological phosphorus removal process. *Biotechnol Bioeng*. 1995;47:277–287.
2. Kuba T, Murnleitner E, van Loosdrecht MCM, Heinen JJ. A metabolic model for the biological phosphorus removal by denitrifying organisms. *Biotechnol Bioeng*. 1996;52:685–695.
3. Brdjanovic D, van Loosdrecht MCM, Versteeg P, Hooijmans CM, Alaerts GJ, Heijnen JJ. Modeling COD, N and P removal in a

full scale WWTP Haarlem Waarderpolder. *Water Res.* 2000;34: 846–858.
4. Meijer SCF, van Loosdrecht MCM, Heijnen JJ. Modeling the start-up of a full-scale biological phosphorous and nitrogen removing WWTP. *Water Res.* 2002;36:4667–4682.
5. de Kreuk MK, Picioreanu C, Hosseini M, Xavier JB, van Loosdrecht MCM. Kinetic model of a granular sludge SBR: influences on nutrient removal. *Biotechnol Bioeng*. 2007;97:801–815.
6. Siegrist H, Vogt D, Garcia-Heras JL, Gujer W. Mathematical model for meso- and thermophilic anaerobic sewage sludge digestion. *Environ Sci Technol*. 2002;36:1113–1123.
7. Sin G, Guisasola A, de Pauw DJW, Baeza JA, Carrera J, Vanrolleghem PA. A new approach for modelling simultaneous storage and growth processes for activated sludge systems under aerobic conditions. *Biotechnol Bioeng*. 2005;92:600–613.
8. Grady CPL Jr, Daigger GT, Lim HC.*Biological Wastewater Treatment. Revised and Expanded*, *2nd ed.* New York: Marcel Dekker, 1999.
9. Sahlstedt KE, Aurola AM, Fred T. Practical modelling of a large activated sludge DN-process with ASM3. Proceedings of the Ninth IWA Specialized Conference on Design, Operation and Economics of Large Wastewater Treatment Plants, 1-4 September 2003, Praha, Czech Republic, 2003:141–148.
10. Wichern M, Lubken M, Blomer R, Rosenwinkel KH. Efficiency of the Activated Sludge Model no. 3 for German wastewater on six different WWTPs. *Water Sci Technol*. 2003;47:211–218.
11. Gernaey KV, van Loosdrecht MCM, Henze M, Lind M, Jørgensen SB. Activated sludge wastewater treatment plant modelling and simulation: state of the art. *Environ Modelling Software*. 2004;19:763–783.
12. Henze M, Gujer W, Mino T, van Loosdrecht MCM.*Activated Sludge Models ASM1, ASM2, ASM2d, and ASM3*. IWA Scientific and Technical Report No. 9. London, UK: IWA Publishing, 2000.
13. Henze M, Grady CPL Jr, Gujer W, Marais GVR, Matsuo T. *Activated Sludge Model No. 1. Scientific and Technical Report No. 1*. London: IAWPRC, 1987.
14. Gujer W, Henze M, Mino T, van Loosdrecht MCM. Activated sludge model No. 3. *Water Sci Technol*. 1999;39:183–193.
15. Rieger L, Koch G, Kuhni M, Gujer W, Siegrist H. The EAWAG bioP-module for activated sludge model No. 3. *Water Res.* 2001;35: 3887–3903.
16. Sin G, Kaelin D, Kampschreur MJ, Takacs I, Wett B, Gernaey KV, Rieger L, Siegrist H, van Loosdrecht MCM. Modelling nitrite in wastewater treatment systems: a discussion of different modelling concepts. *Water Sci Technol*. 2008;58:1155–1171.
17. Ni BJ, Yu HQ. An approach for modeling two-step denitrification in activated sludge systems. *Chem Eng Sci.* 2008;63:1449–1459.
18. Gujer W, Larsen TA. The implementation of biokinetics and conservation principles in ASIM. *Water Sci Technol*. 1995;31:257–266.
19. Insel G, Celikyilmaz G, Ucisik-Akkaya E, Yesiladali K, Cakar ZP, Tamerler C, Orhon D. Respirometric evaluation and modeling of glucose utilization by *Escherichia coli* under aerobic and mesophilic cultivation conditions. *Biotechnol Bioeng*. 2007;96:94–105.
20. Henze M, Gujer W, Mino T, Matsuo T, Wentzel MC, Marais GR, van Loosdrecht MCM. Activated sludge model No. 2d. *Water Sci Technol*. 1999;39:165–182.
21. Mino T, van Loosdrecht MCM, Heijnen JJ. Review paper: microbiology and biochemistry of the enhanced biological phosphate removal process. *Water Res.* 1998;32:3193–3207.
22. Satoh H, Ramey WD, Koch FA, Oldham WK, Mino T, Matsuo T. Anaerobic substrate uptake by the enhanced biological phosphorus removal activated sludge treating real sewage. *Water Sci Technol*. 1996;34:9–16.
23. Thomsen JK, Geest T, Cox RP. Mass spectrometric studies of the effect of pH on the accumulation of intermediates in denitrification by *Paracoccus denitrificans*. *Appl Environ Microbiol*. 1994;60:536–541.
24. Sozen S, Orhon D. The effect of nitrite correction on the evaluation of the rate of nitrate utilization under anoxic conditions. *J Chem Technol Biotechnol*. 1999;74:790–800.
25. Oh J, Silverstein J. Acetate limitation and nitrite accumulation during denitrification. *J Environ Eng*. 1999;125:234–242.
26. Henze M, Gujer W, Mino T, Matsuo T, Wentzel MC, Marais GR. *Activated Sludge Model No. 2*. IAWQ Scientific and Technical Report No. 3. London U.K.: IAWQ, 1995:32.
27. APHA.*Standard Methods for the Examination of Water and Wastewater. 19th ed.* Washington, DC: American Public Health Association, 1995.
28. Wentzel MC, Mbewe A, Lakay MT, Ekama GA. Batch test for characterization of the carbonaceous materials in municipal wastewaters. *Water SA*. 1999;25:327–335.
29. Roeleveld PJ, van Loosdrecht MCM. Experience with guidelines for wastewater characterisation in The Netherlands. *Water Sci Technol*. 2002;45:77–87.
30. Makinia J, Rosenwinkel KH, Spering V. Long-term simulation of the activated sludge process at the Hanover-Gummerwald pilot WWTP. *Water Res.* 2005;39:1489–1502.
31. Reichert P.*Aquasim 2.0-User Manual, Computer Program for the Identification and Simulation of Aquatic Systems*.Dübendorf, Switzerland: EAWAG, (ISBN 3 906484 16 5), 1998.
32. Koch G, Kuhni M, Gujer W, Siegrist H. Calibration and validation of activated sludge model No. 3 for Swiss municipal wastewater. *Water Res.* 2000;34:3580–3590.
33. Hu Z, Wentzel MC, Ekama GA. A general model for biological nutrient removal activated sludge systems: model development. *Biotechnol Bioeng*. 2007;98:1242–1258.
34. Hu Z, Wentzel MC, Ekama GA. A general model for biological nutrient removal activated sludge systems: model evaluation. *Biotechnol Bioeng*. 2007;98:1259–1275.
35. Still DA, Ekama GA, Wentzel MC, Casey TG, Marais GR. Filamentous organism bulking in nutrient removal activated sludge systems. Paper 2: Stimulation of the selector effect under aerobic conditions. *Water SA*. 1996;22:97–118.
36. Krishna C, van Loosdrecht MCM. Substrate flux into storage and growth in relation to activated sludge modelling. *Water Res.* 1999; 33:3149–3161.
37. Moussa MS, Hooijmans CM, Lubberding HJ, Gijzen HJ, van Loosdrecht MCM. Modelling nitrification, heterotrophic growth and predation in activated sludge. *Water Res.* 2005;39:5080–5098.

Manuscript received Feb. 17, 2009, revision received Jun. 15, 2009, and final revision received Aug. 11, 2009.